ORIGINAL ARTICLE

TGFβ1 induces epithelial–mesenchymal transition, but not myofibroblast transdifferentiation of human kidney tubular epithelial cells in primary culture

Monica Forino[*], Rossella Torregrossa[*], Monica Ceol[*], Luisa Murer[†], Manuela Della Vella[†], Dorella Del Prete[*], Angela D'Angelo[*] and Franca Anglani[*]

[*]Laboratory of Histomorphology and Molecular Biology of the Kidney, Division of Nephrology, Department of Medical and Surgical Sciences, University of Padua, Padova, Italy, and [†]Department of Pediatrics, University of Padua, Padova, Italy

Summary

The origin and fate of renal interstitial myofibroblasts (MFs), the effector cells of renal fibrosis, are still debated. Experimental evidence suggests that renal MFs derive from tubular epithelial cells throughout the epithelial–mesenchymal transition (EMT) process. Primary human tubular epithelial cells (HUTECs) were cultured for 4 and 6 days on plastic or type I collagen-coated plates with 1, 5, 10 and 50 ng/ml of transforming growth factor β1 (TGFβ1). The EMT process was monitored by morphology and immunophenotyping for αSMA, cytokeratin 8–18, E-cadherin, vimentin and collagen III. Quantitative comparative RT/PCR and real-time PCR were used to evaluate the expression of collagen III and IV, fibronectin, tenascin, MMP-2, CTGF, E-cadherin and cadherin 11 genes, as well as those of the Smad signalling pathway. TGFβ1 was found capable of reactivating the mesenchymal programme switched off during tubulogenesis, but it induced no *de novo* expression of αSMA gene or myofibroblast phenotype. We demonstrate that the EMT process is conditioned by the extracellular matrix and characterized by TGFβ1-driven Smad3 downregulation. Our study results suggest that TGFβ1 could function as a classic embryonal inducer, initiating a cascade of de-differentiating events that might be further controlled by other factors in the cellular environment.

Keywords

epithelial–mesenchymal transition, gene expression, human tubular epithelial cells, myofibroblasts, Smad signalling, transforming growth factor β1

The progression of most kidney diseases towards end-stage renal failure is related to pathological changes in the renal interstitium. Early histomorphological signs of interstitial fibrosis (IF) in renal biopsies are associated with an unfavourable prognosis, even if routine clinical parameters still indicate a compensated kidney function (Mackensen-Haen *et al.* 1992). IF is characterized by the appearance of fibroblasts that are often positive for alpha smooth muscle actin (αSMA) microfilaments (myofibroblasts) in damaged areas. This phenomenon seems to be strongly associated with progression

of the nephropathy towards kidney failure (Badid *et al.* 2000; Badid *et al.* 2002). While the role of myofibroblasts in renal fibrosis is widely accepted, their origin and fate are still a matter of debate (Liu 2004). Since the pioneering study by Strutz *et al.* (1995), evidence from both *in vivo* and *in vitro* models suggests that the renal interstitial cells' acquisition of the αSMA phenotype may be secondary to the epithelial-to-mesenchymal transdifferentiation (EMT) of tubular epithelial cells. Transdifferentiation classically refers to differentiated cells changing into other differentiated cells, i.e. the acquisition of a new phenotype by a differentiated cell (Tosh & Slack 2002). It is not yet clear whether the mesenchymal transition of renal tubular cells is a transient phase of the transdifferentiating epithelium or whether EMT producing fibroblasts is an arrested form of transdifferentiation. Indeed, the tubular epithelial to myofibroblast transdifferentiation (TEMT) phenomenon was recently reviewed by Lan (2003) and found to occur both *in vivo* in the remnant kidney model (Ng *et al.* 1998) and *in vitro* under transforming growth factor β1 (TGFβ1) or glycated albumin stimulus (Fan *et al.* 1999; Oldfield *et al.* 2001). TEMT was also demonstrated in human kidneys, both *in vivo* (Jinde *et al.* 2001; Rastaldi *et al.* 2002) and *in vitro*, in the SV40-immortalized human cell line HKC-8 (Yang & Liu 2001). These data seem to support the hypothesis that EMT is indeed a transitional phase towards the myofibroblast phenotype. A recent elegant study by Iwano *et al.* (2002) has provided compelling evidence that a large proportion (36%) of interstitial fibroblasts in fibrotic renal tissue derive from proximal tubular cells, thus emphasizing that the contribution of the EMT pathway to renal fibrosis is far greater than that was previously thought. No mention was made of tubular epithelial to myofibroblast transdifferentiation in this model, however.

Little is known of the genetic switch responsible for the tubular cells' acquisition of the αSMA phenotype. TGFβ1 is a key modulator of the myofibroblast phenotype in fibroblasts during the wound-healing process (Desmouliere *et al.* 1993), and in mesangial cells in culture (Johnson *et al.* 1992). But TGFβ1 is also capable of inducing EMT in a variety of epithelial cells, including renal tubular epithelial cells (Tian *et al.* 2003).

TGFβ1-induced EMT appears to depend primarily on an intact Smad signalling (Flanders 2004; Zavadil *et al.* 2004). Receptor activation leads to phosphorylation and activation of the receptor-regulated Smads, Smad2 and Smad3. They form complexes with the common mediator Smad, Smad4, that accumulate in the nucleus and are directly involved in the transcriptional activation of target genes, usually in conjunction with other transcription factors (Massaguè & Wotton 2000).

Conversely, the growth factor BMP-7 counteracts TGFβ1-induced EMT by enhancing E-cadherin expression via Smad5, thus restoring the epithelial phenotype (Zeisberg *et al.* 2003).

Our previous study results (Forino *et al.* 1997; Anglani *et al.* 1998) indicate that primary human tubular epithelial cells cultured on plastic have a transitional phenotype because they co-express vimentin and cytokeratin microfilaments, and they express αSMA mRNA and protein, albeit in the presence of both a clear cobble-stone morphology (typical of epithelial cells) and E-cadherin-positive cells. We hypothesized that this transitional phenotype, probably due to disruption of the basal tubular membrane and a partial loss of cellular adhesion properties, could be directed by TGFβ1 to a myofibroblast phenotype. Using primary human tubular epithelial cells (a more physiological system than transformed cell lines), we demonstrate that TGFβ1 can induce morphological, molecular and biochemical changes towards a more definite mesenchymal phenotype, but it gives rise to no *de novo* expression of αSMA gene or myofibroblast phenotype. We also show that the EMT process is conditioned by the extracellular matrix and characterized by TGFβ1-driven Smad3 downregulation.

Materials and methods

Tubular epithelial cell isolation and culture

Primary HUTEC cultures were established as described elsewhere, with minor modifications (Lin *et al.* 1993). Briefly, histologically normal human renal cortexes were obtained from surgical biopsies taken subject to informed consent in paediatric patients undergoing surgery for extrinsic pyeloureteral obstruction. The cortexes were minced and pressed through a 224-μm stainless steel mesh, then separated into glomerular and tubular fractions by serial retention on 106 and 45-μm meshes, respectively. The tubular fraction was cultured in selective medium consisting of Minimum Essential Medium Eagle D-Valine modification (MEM-D-Val, Sigma, St Luis, MO, USA), 10 mM HEPES buffer pH 7.3, 50 μM 2-mercaptoethanol, 100 μg/ml of ampicillin, 100 μg/ml of streptomycin, 30 nM insulin–transferrin–sodium selenite (Sigma), 30 nM tri-iodiothyronine (Sigma) and 50 nM hydrocortisone (Sigma) in 25-cm² flasks (Falcon BD, Franklin Lakes, NJ, USA). Confluent cultures were split 1:3 as necessary using trypsin EDTA. Immunocytochemical techniques were used to detect the presence of the epithelial intracellular marker cytokeratin, and the absence of factor VIII, in each cell preparation. All cells were cytokeratin-positive and factor VIII-negative. Cytochemistry was used to demonstrate pea lectin binding of tubular cells using

peroxidase-bound lectins. Gamma-glutamyl transferase activity was tested using γ-glutamyl-4-methoxy-2-naphthylamide as a substrate. These methods enabled us to determine that the majority of the starting cell population was of proximal tubular origin.

Cells at passage 1 were used for TGFβ1 stimulation experiments, designed to simultaneously monitor the effect of TGFβ1 at both phenotypic and molecular levels. Cells were seeded at subconfluence and incubated at 37 °C in a 5% CO_2 atmosphere for 24 h under quiescent conditions (1% FCS in RPM1-1640) both in 6-well plastic or collagen I-coated plates for RNA extraction and in 8-chamber plastic or collagen I-coated slides for immunophenotyping. Cells were then cultured for 4 and 6 days in the presence of 1, 5, 10 and 50 ng/ml of human TGFβ1 (Prepro Tech EC, London, UK). Control conditions were represented by cells maintained for 4 and 6 days in 1% serum without TGFβ1. This strategy was used because we were confident that the results obtained in the same experimental setting would enable us to observe TGFβ1 effects simultaneously from three different standpoints, i.e. the biochemical, the molecular and the phenotypic, thus avoiding confounding factors due to different passages or different local culture conditions.

Timecourse experiments were also performed, utilizing a different renal tubular cell isolate, with 1 ng/ml of TGFβ1 for 1–6 days. To test the efficacy of TGFβ1 treatment in inducing myofibroblast phenotype in our culture conditions, primary human dermal fibroblasts at passage 2 were used as control cells, run in parallel with the primary HUTECs and treated in the same way.

Fresh TGFβ1 was added to the cultures every 2 days, changing half of the medium. Cells were seeded at the same concentration and analysed at the same time to obtain a similar degree of subconfluence in each plate. When cells were incubated with TGFβ1 for 1, 2, ..., *n* days, this means that the cells remained under 1% FCS for 6–1, 6–2, ..., 6–*n* days.

Control conditions were established by culturing cells (i) without TGFβ1 in 1% serum and (ii) with 1 and 50 ng/ml of TGFβ1, 4 and 5 or 10 μg/ml of a neutralizing polyclonal rabbit anti-TGFβ1 antibody (Promega, Madison, WI, USA).

Cellular morphology analysis and immunophenotyping

HUTECs cultured on both collagen- and plastic-coated 8-chamber slides, with or without TGFβ1, were stained with monoclonal and polyclonal antibodies against αSMA (clone asm 1 – Boheringer Mannheim, Germany), cytokeratin 8–18 (BioGenex, San Ramon, CA, USA), vimentin (clone V9, DAKO, Glostrup, Denmark), collagen III (Southern

Biotechnology Associates, Birmingham, AL, USA), Ki67 (clone MB1, DAKO) **and** E-cadherin (TAKARA Biomedicals, Shiga, Japan). Cells were fixed in ice-cold acetone for 5 min, pre-incubated with 1% BSA and then incubated with the specific antibody overnight at 4 °C. After washing with PBS, endogenous peroxidase was inactivated by 20-min incubation in 0.3% H_2O_2 in methanol. Slides were subsequently incubated with peroxidase-conjugated anti-mouse IgG and peroxidase-conjugated antiperoxidase complexes (PAP) and then developed with 3-3-diaminobenzidine (DAB, DAKO) to produce a brown-coloured signal. Cells were counterstained with haematoxylin and mounted in aqueous medium.

Slides were blinded for identity. Immunopositivity was quantified by counting the number of positively stained cells in at least 100 cells under 200× magnification. Signal intensity in each field was also recorded from weak (+/−) to intense (+++).

mRNA profiling

Quantitative comparative RT/PCR was used to analyse the expression profile of genes belonging to the mesenchymal and epithelial genetic programme, including growth factors (connective tissue growth factor, CTGF), matrix proteins (collagen type III, fibronectin, tenascin and MMP-2), basal membrane proteins (collagen type IV) and cellular adhesion molecules (E-cadherin and cadherin 11). αSMA expression was also specifically analysed in both the dose-dependent and the timecourse experiments to assess the TGFβ1-driven αSMA regulation at transcriptional level.

Real-time PCR was used to investigate Smad-dependent TGFβ1 and BMP-7 signalling during EMT.

Quantitative comparative RT/PCR

Total RNA was extracted using RNAzolB (BIOTEX, Houston, TX, USA) according to the protocol. Approximately 200 ng of total RNA purified from the aqueous phase was retrotranscribed in a total volume of 20 μl containing 5 mM $MgCl_2$, 1 mM dNTPs (Boheringer), 2.5 μM random hexamers (Perkin Elmer, Branchburg, NJ, USA), 1 U Rnase inhibitor (Perkin Elmer) and 2.5 U MuLV reverse transcriptase (Perkin Elmer) in a buffer of 50 mM KCl and 10 mM Tris–HCl pH 8.3. The reaction was performed at 42 °C for 30 min and at 99 °C for 5 min in a thermal cycler (MJ Research, Watertown, MA, USA). An aliquot of 2 μl of the RT reaction was used to amplify each of the nine genes in a final volume of 25 μl containing 1.5 mM $MgCl_2$, 0.2 mM dNTPs, 0.4 μM specific primers, 2 U JumpStart Taq (Sigma)

in 50 mM KCl and 10 mM Tris–HCl pH 8.3. The amplification profile was the same for each primer set and consisted of 45 s at 94 °C, 45 s at 60 °C and 2 min at 72 °C. PCR amplification of glyceraldehyde-3-phosphate dehydrogenase (G3PDH) was also performed as an internal standard. We applied the RT/PCR kinetic strategy described elsewhere (Ceol *et al.* 2001) to obtain quantitative data. The specific cycle numbers and primer sequences are summarized in Table 1. Gel bands were quantified by densitometric analysis using GEL-PRO ANALYSER software (Media Cybernetics, Silver Spring, MD, USA). The relative level of each mRNA was obtained by calculating the ratio of the target gene to the G3PDH optical densities (OD).

The reproducibility of our RT/PCR approach was tested by performing two RT/PCR of αSMA gene under each experimental condition and calculating the linear regression (interassay variability): on collagen, $r = 0.940$ with $P = 0.017$ and on plastic, $r = 0.933$ with $P = 0.020$. The precision of the procedure was also tested by performing four RT/PCR of the same sample and determining the coefficient of variation (CV) (intra-assay variability), which varied from 20 to 56%.

Real-time PCR

Real-time PCR was used to quantify the expression of Smad3, Smad4, Smad5 and BMP-7 mRNAs. G3PDH mRNA was also evaluated as an internal standard. Real-time PCR was performed using the iCycler Thermal Cycler (BioRad Hercules, CA, USA) and SYBR Green I technology.

The specific sets of primers were designed by BEACON DESIGNER PROBE/PRIMER DESIGN software (BioRad). Primer sequences and amplicon size are given in Table 2. The optimal conditions for the primers (300 nml/l) and MgCl$_2$ (3 mmol/l) were determined in preliminary experiments.

The PCR standards for Smads and BMP-7 consisted of known numbers of molecules of purified PCR products. After checking the specificity by PAGE analysis, the PCR products were purified using MinElute PCR Purification Kit (Qiagen, Hilden, Germany) and quantified by spectrophotometry at a wavelength of 260 nm.

The number of copies/millilitre of the standards was calculated according to the following formula:

$$\text{copies/ml} = 6.023 \times 10^{23} \times C \times OD^{260}/MWt$$

where $C = 5 \times 10^{-5}$ g/ml for DNA and MWt = molecular weight of PCR product gene (base pairs $\times 6.58 \times 10^2$ g).

Standards were serially diluted in 1:2, 1:4 or 1:10 log steps, from 10^8 down to 10 copies. All calibration curves for purified PCR products, G3PDH, Smads and BMP-7 were linear over the whole quantification range, with correlation coefficients ranging from $r = 0.998$ to $r = 0.995$, indicating a precise log-linear relationship. The slope of the four standards varied from 3.4 to 3.6 demonstrating comparable PCR amplification efficiencies. The intrarun variability, calculated from triplicate samples for all target genes, showed an average SD for the threshold cycles of 0.18 cycles.

The thermal cycling profile consisted of a step 1 at 95 °C for 5 min and a step 2 at 94 °C for 30 s, followed by 30 s of the appropriate annealing temperature. Step 2 was repeated 40 times for Smads and 50 times for BMP-7. The fluorescence product was detected during annealing/extension periods. As SYBR Green I also binds to primer dimers formed non-specifically during all PCR reactions, a melting curve analysis was used to confirm the specificity of the amplification products, as follows: step 1 at 50 °C for 15 s; step 2 from 50 °C, increasing the temperature by 0.5 °C every 15 s up to a final temperature of 95 °C.

The quantification data were analysed using ICYCLER software and expressed as the ratio of the starting quantity mean (SQm) of the target to the housekeeping gene.

Table 1 RT/PCR primer sequences

Gene	Upstream primer	Downstream primer	Size (bp)	PCR cycles
G3PDH	TGAAGGTCGGAGTCAACGGATTTGGT	CATGTGGGCCATGAGGTCCACCAC	983	24
αSMA	CTGCCTTGGTGTGTGACAAT	ATTGTGGGTGACACCATCTC	470	30
Cadherin 11	GCCAGACACAGTTCTTAAGG	ATCAAACCTGAGTATCAGTA	310	34
E-Cadherin	AGTGCCAACTGGACCATTCA	TCTTTGACCACCGCTCTCCT	350	28
MMP-2	ACCTGGATGCCGTCGTGGAC	TGTGGCAGCACCAGGGCAGC	447	26
α1collagen III	GGACCACCAGGGCCTCGAGGTAAC	TGTCCACCAGTGTTTCCGTG	471	25
α1collagen IV	TTTGCATCACGAAATGACTAC	AAGGTGGACGGCGTAGGCTTC	413	25
Fibronectin	GGACTTCCTATGTGGTCGGA	GTTGGTAAACAGCTGCACGA	312	24
Tenascin	ACTGTGGACGGAACCAAGAC	AGGTAACCGGTGACTGATGC	274	24
CTGF	ACGAGCCCAAGGACCAAA	TTGTAATGGCAGGCACAGG	483	25

Table 2 Real-time PCR primer sequences

Gene	Upstream primer	Downstream primer	Size (bp)	Annealing temperature (°C)
G3PDH	GAAGGTGAAGGTCGGAGT	TGGCAACAATATCCACTTTACCA	92	60
Smad3	ATCTACTGCCGCCTGTGG	TCTCTGGTAGTGGTAGGGATTC	129	64
Smad4	GCCAACTTTCCCAACATTCCTG	TGCTGCTGTCCTGGCTGAG	116	68
Smad5	CTTTCCACCAGCCCAACAACAC	TAGGCAGGAGGAGGCGTATCAG	151	68
BMP-7	GACGCTGGTCCACTTCATCAAC	TGGAGCTGTCATCGAAGTAGAGG	101	60

Statistical analysis

Data were expressed as mean ± SE. The statistical analysis was performed using the *t*-test and linear regression analysis. A *P*-value of ≤0.05 was considered statistically significant.

Results

Morphological and immunocytochemical studies

TGFβ1 is a known inhibitor of epithelial cell proliferation. Primary cultures of HUTEC were examined for their response to TGFβ1. Following exposure to TGFβ1, cells did not proliferate as revealed by negative immunostaining for Ki67, a well-known marker of cell proliferation. A drastic alteration in cell shape, however, was observed: under the light microscope, untreated cells displayed the characteristic cuboidal shape of epithelial cells, but after TGFβ1 treatment, they were elongated and spindle shaped, with front-end to back-end polarity, i.e. fibroblast-like. The effect was already apparent after 24 h with only 1 ng/ml of TGFβ1 and was dose-dependent and more evident on the collagen-coated surface (Figure 1). TGFβ1 was prevented from inducing the fibroblast phenotype by the addition of a neutralizing anti-TGFβ1 antibody (data not shown).

We then tested whether this change in HUTEC morphology correlated with the disappearance of epithelial and the appearance of mesenchymal markers, including αSMA. We examined cytokeratin and E-cadherin as epithelial markers. All of the control cells were cytokeratin-positive. On plastic, 4 and 6 days of TGFβ1 treatment did not make the cytokeratin disappear, however, despite the clearly fibroblastic morphology. On collagen, the downregulating effect of TGFβ1 was only evident at 4 days, as cytokeratin downregulation at 6 days was attributable to the influence of the matrix. In fact, both control and treated cells displayed a very faint but persistent positivity at 6 days (Figure 2).

In untreated samples, 30% of the cells were E-cadherin immunopositive on collagen and 60% on plastic after 4 days, indicating the influence of the matrix on cadherin expression. After 6 days, said immunopositivity disappeared in control conditions and TGFβ1 treatment had no effect on E-cadherin phenotype (data not shown).

To characterize the fibroblastic, and possibly myofibroblastic phenotype of the treated cells, we determined the expression of the mesenchymal markers vimentin, collagen III and αSMA. Vimentin immunopositivity was detected in 100% of the control cells at 4 days and was intense on plastic but weak on collagen. TGFβ1 treatment had no effect on the intensity of vimentin signal of the cells grown on plastic but induced it to increase on collagen. After 6 days of culture, however, the signal intensity and the number of positive cells decreased in the treated cells (Figure 3). TGFβ1-driven downregulation of the vimentin cytoskeleton was confirmed in three different experiments. Collagen III immunodeposition was found to parallel vimentin immunodeposition (data not shown) and was high in the treated cells at 4 days, but low at 6 days.

Cells expressing αSMA microfilaments were not detected in either control or treated cells both on collagen and plastic surface (data not shown). On plastic, the highest TGFβ1 (50 ng/ml) dosage for 6 days also caused cell hypertrophy and hillock formation, and αSMA-positive vesicles were detected in rare cells, often with a perinuclear localization, and occasionally extending to the cytoplasm.

mRNA profiling of EMT

To further characterize the tubular cells' mesenchymal transition, we analysed the HUTEC expression profile for genes belonging to the mesenchymal (CTGF, cadherin 11, collagen III, fibronectin, tenascin and MMP-2) and epithelial (E-cadherin and collagen IV) genetic programmes. After 4 days of culture, a clearly TGFβ1-induced and dose-dependent increase in mesenchymal markers was evident both on the collagen-coated and on the plastic surfaces. On collagen (Figure 4), the effect was most pronounced for collagen III and MMP-2 (at 50 ng/ml, it was a nine- and 11-fold increase over controls, respectively), but tenascin, fibronectin and cadherin 11 mRNAs were also upregulated by TGFβ1
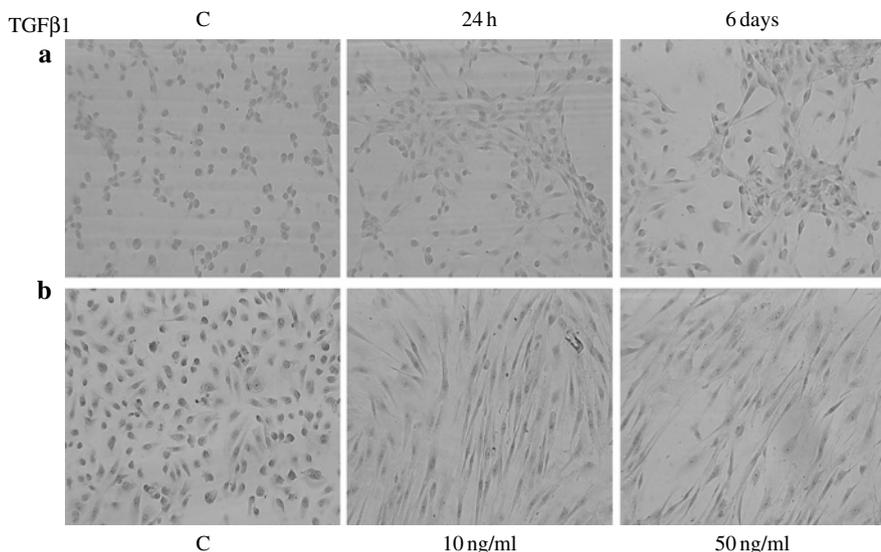
Figure 1 TGFβ1-driven epithelial to mesenchymal transformation in primary HUTEC. (a) Morphological changes induced by 1 ng/ml of TGFβ1 for 24 h and 6 days on plastic surfaces. (b) Morphological changes induced by 10 and 50 ng/ml of TGFβ1 for 6 days on collagen-coated surfaces. C, control condition. Magnification: 100×.

(two- to seven-fold over controls at 50 ng/ml). On the plastic surface (Figure 5), the effect of TGFβ1 was more dramatic: on collagen III and MMP-2 from 40- to 100-fold and on tenascin, fibronectin and cadherin 11 from six- to 11-fold over controls at 50 ng/ml. The connective tissue growth factor (CTGF) mRNA was also upregulated threefold in the presence of 50 ng/ml of TGFβ1 both on collagen and on plastic.

Regression analysis was applied to further confirm the TGFβ1-driven mesenchymal marker upregulation. On both collagen and plastic, a significant and very close correlation
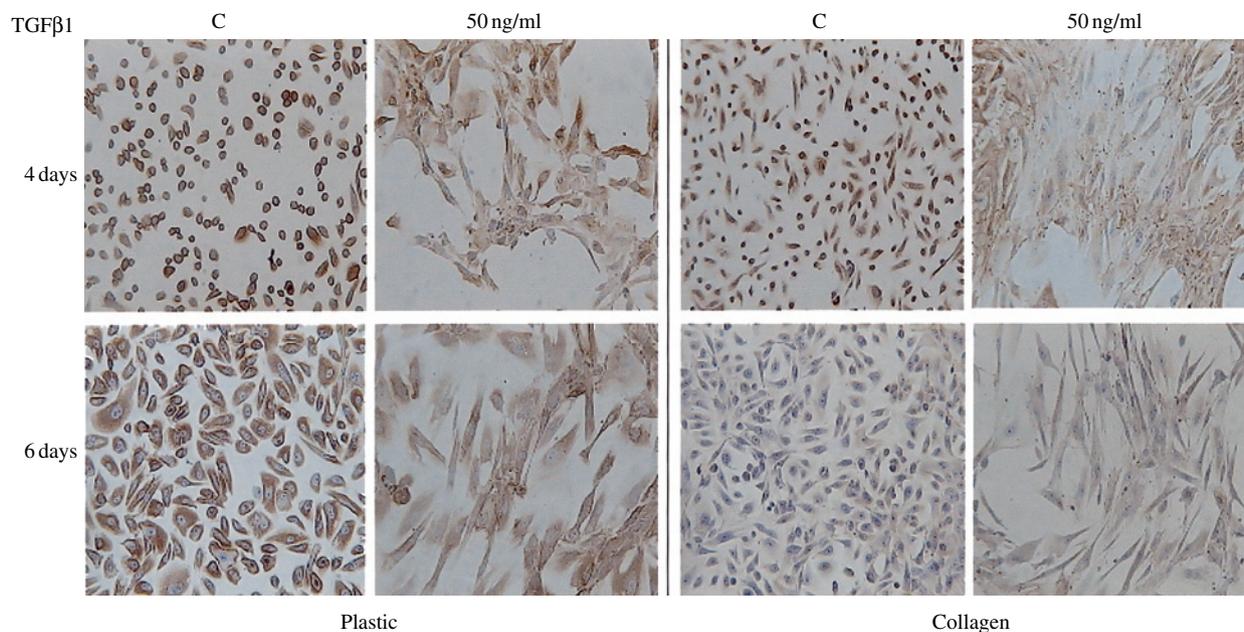

Figure 2 Cytokeratin immunostaining of HUTEC after TGFβ1 treatment for 4 and 6 days. In control conditions (C), primary HUTEC were all cytokeratin-positive. The signal is more intense on plastic surface, and at 6 days, the cells are also hypertrophic. After 50 ng/ml of TGFβ1 treatment for 6 days, the majority of cells appear elongated with a front-end to back-end polarity, suggestive of a mesenchymal phenotype; cytokeratin immunodeposition is still present, and intense, and involves 80% of the cells on the plastic surface, whereas it is very weak but still involving 70% of cells on collagen surface. At 4 days of treatment, a reduced cytokeratin immunodeposition is visible only on collagen-coated surfaces, where some elongated cells are already negative. Magnification: 100×. The figures and percentages are representative of findings in three experiments.
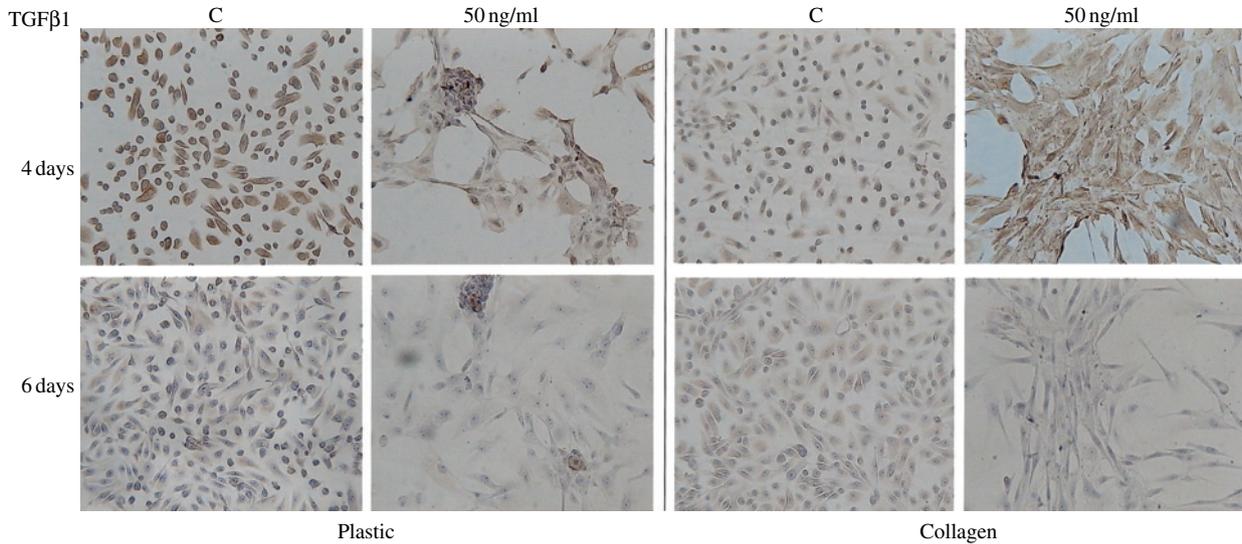
Figure 3 Vimentin immunophenotyping of HUTEC after TGFβ1 treatment for 4 and 6 days. C: control condition. On a plastic surface, under serum-free conditions (C), at day 4 and day 6, 100 and 50% of the cells, respectively, are positive. Different dosages of TGFβ1 after 4 days do not modify the number and the signal intensity of positive cells, whereas after 6 days at 50 ng/ml the number of positive cells and the staining intensity are reduced. On a collagen surface under serum-free conditions (C), at day 4 and day 6, 100 and 80% of cells, respectively, are positive, but the signal is weak. TGFβ1-treated cells on day 4 show a higher signal intensity than control cells, whereas on day 6 the cells become negative as the dosage increased. Magnification: 100×. The figures and percentages are representative of the results of three experiments.

was found between mRNA level and TGFβ1 dosage for CTGF ($r = 0.96$, $P = 0.007$ on plastic; $r = 0.91$, $P = 0.03$ on collagen) and cadherin 11 ($r = 0.91$, $P = 0.03$ on plastic; $r = 0.89$, $P = 0.03$ on collagen), and a near-significant correlation was found for tenascin, MMP-2 and collagen III (range $r = 0.87$–0.73, $P = 0.05$–0.1).

Conversely, E-cadherin, which was downregulated in an apparently dose-dependent manner, did not correlate with TGFβ1 dosage and correlated inversely with cadherin 11 ($r = 0.82$, $P = 0.05$).

TGFβ1 treatment did not affect αSMA mRNA expression. It was only at 4 days on collagen, and 6 on plastic that there was a slight, but not significant, decrease and increase, respectively (Figure 6).

Using real-time PCR analysis, we studied the gene expression of both Smad3, Smad4 and Smad5 and the counteracting
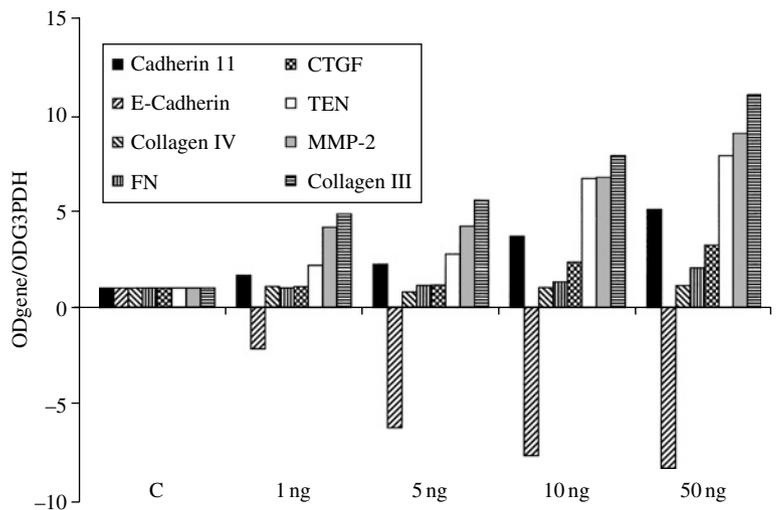

Figure 4 mRNA profiling by RT/PCR of TGFβ1-treated primary HUTEC grown on a collagen-coated surface for 4 days. mRNA levels are reported as target gene/G3PDH ratio and normalized to control (C). This is one of two experiments producing similar results.
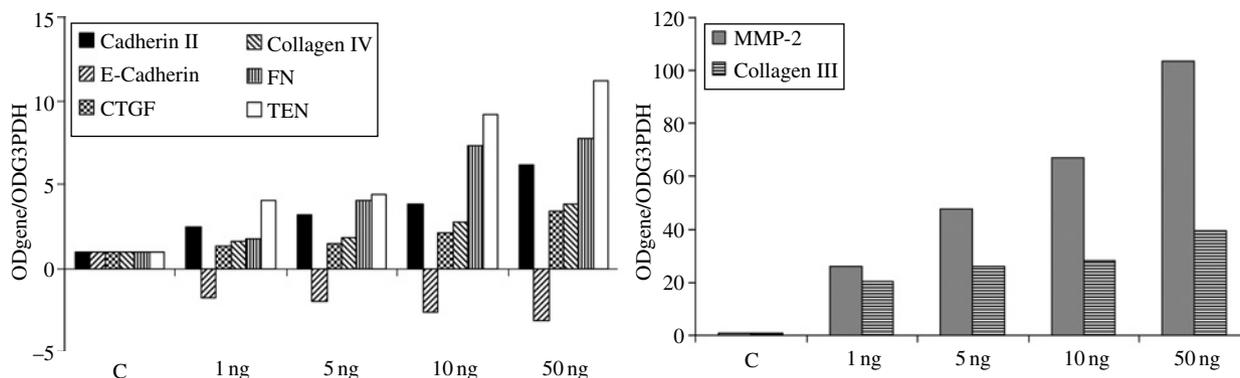
Figure 5 mRNA profiling by RT/PCR of TGFβ1-treated primary HUTEC grown on a plastic surface for 4 days. mRNA levels are reported as target gene/G3PDH ratio and normalized to control (C). This is one of two experiments producing similar results.

BMP-7 throughout EMT transition of HUTEC. Smad3 transcriptional levels were lowered by TGFβ1 in an apparently dose-dependent manner both at 4 and at 6 days of treatment (Figure 7a), whereas Smad4 levels were constantly high throughout the EMT transition. Very low levels of BMP-7 mRNA were found on both collagen and plastic after 6 days of treatment at all dosages except for 50 ng/ml of TGFβ1 on plastic, where a marked but not significant upregulation was seen. Smad5 expression at 6 days on collagen was high, whereas it was downregulated in an apparently dose-dependent manner on plastic (Figure 7b).

αSMA expression in timecourse experiments

To try and understand how αSMA expression is regulated at transcriptional and post-transcriptional levels in renal epithelial cells under TGFβ1 stimulus, we performed timecourse experiments (from 1 to 6 days) using 1 ng/ml of TGFβ1 (Figure 8). Primary cultures of human dermal fibroblasts and HUTEC were run in parallel under the same culture conditions (RPM1-1640, 1% FCS on a plastic surface). Immunocytochemical analysis revealed that 1 ng/ml of TGFβ1 for 24 h was sufficient to make 50% of fibroblasts acquire the αSMA phenotype; at 6 days, 100% of the cells

were myofibroblasts (Figure 8b, B). The appearance of the myofibroblast phenotype was accompanied by an upregulation of αSMA mRNA (with a 2.5-fold increase over controls) (Figure 8a). From day 2–6, there was a drop in αSMA mRNA, but the number of cells with αSMA microfilaments increased. Conversely, TGFβ1 treatment induced a slight increase in αSMA mRNA in HUTEC, with a two-fold increase, at most, over the unstimulated cells after 5–6 days; this was not accompanied by any appearance of the αSMA phenotype (Figure 8b, A).

Discussion

This study demonstrated that TGFβ1 can induce EMT in human renal tubular cells in primary culture. Besides the change in cell morphology, the transition was characterized by a markedly upregulated expression of a number of mesenchymal markers, including CTGF, cadherin 11, fibronectin, tenascin, collagen III and MMP-2, with a parallel drop in the expression of the epithelial markers E-cadherin and cytokeratin. Selective fibroblast proliferation was excluded for two main reasons: cells did not proliferate, and in control conditions, cells were all cytokeratin-positive. We did not measure cell death, but cell density after 6 days of treatment
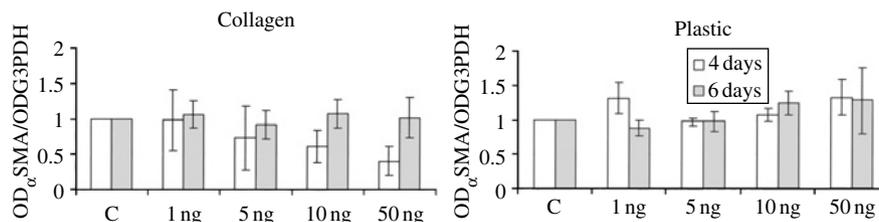

Figure 6 RT/PCR analysis of αSMA mRNA in TGFβ1-treated primary HUTEC on collagen-coated and plastic surfaces. mRNA level is reported as αSMA/G3PDH ratio and normalized to control (C). Means ± SD of four experiments are reported.
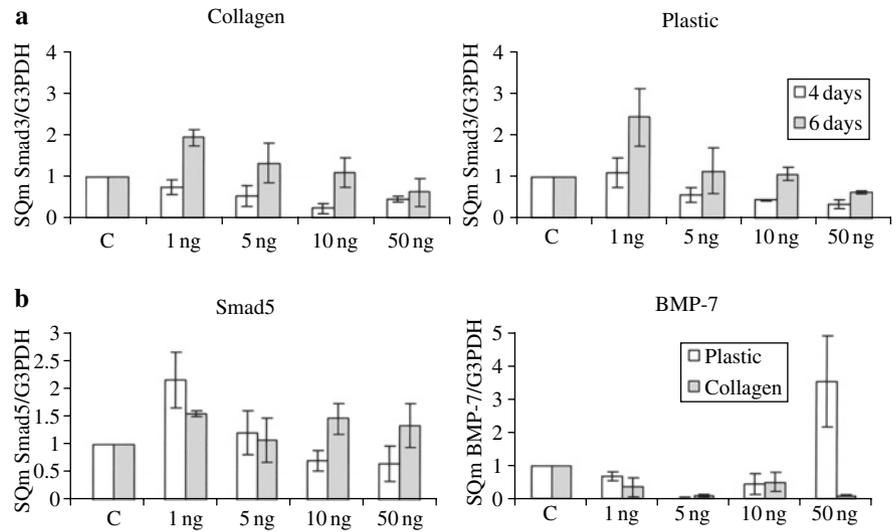
Figure 7 (a) Quantification of Smad3 mRNA level by real-time PCR in TGFβ1-treated primary HUTEC on collagen-coated and plastic surfaces. (b) Quantification of Smad5 and BMP-7 mRNA level by real-time PCR in TGFβ1-treated primary HUTEC grown for 6 days on collagen-coated and plastic surfaces. Means ± SD of three experiments are reported.

did not seem to be changed in respect to control conditions. This transition is a dose-dependent process favoured by cell growth on collagen I. The phenomenon was also evident on plastic but was accompanied by a slight decrease in cytokeratin immunodeposition.

In our model, TGFβ1 downregulates the vimentin cytoskeleton. This was evident after 6 days of treatment, particularly on collagen-coated surfaces, and was demonstrated in three different experiments. Collagen III immunodeposition paralleled vimentin immunophenotyping.

Keeping the HUTEC under low serum conditions on plastic also caused a lesser expression of vimentin microfilaments. Vimentin and cytokeratin microfilaments are normal constituents of the renal tubular cell cytoskeleton when cells are cultured on a plastic surface in 10% FCS (Forino *et al*. 1997;

Baer *et al*. 1999; Friedlander *et al*. 1999), but serum deprivation and starvation caused a reduction in vimentin immunodeposition (personal observation). These observations suggest that the vimentin phenotype in tubular epithelial cells is associated with a proliferative behaviour. This is consistent with studies on acute tubular necrosis induced by toxic or ischaemic injury, in which transient high levels of vimentin expression are seen in tubules during the regenerative phase (Zhu *et al*. 1996). Cytokeratin- and vimentin-negative tubular cells have been observed in dysplastic kidneys (Murer *et al*. 1998).

In our *in vitro* model, E-cadherin phenotype is influenced by both matrix and serum deprivation. In fact, in untreated samples, the number of positive cells was lowered by growing on collagen I and for 6 days.
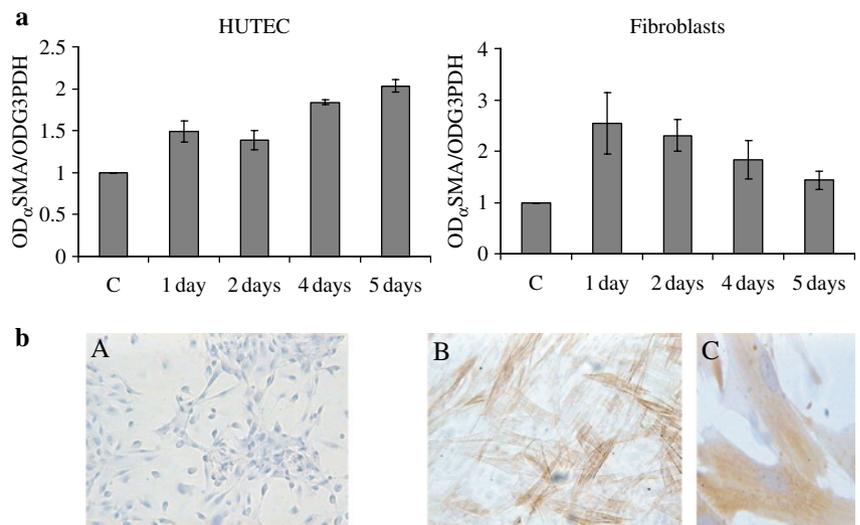

Figure 8 (a) Analysis of αSMA expression by RT/PCR in primary fibroblasts and HUTEC treated with 1 ng/ml of TGFβ1 for 1–5 days on a plastic surface. mRNA level is reported as αSMA/G3PDH ratio and normalized to control, C. (b) αSMA immunostaining of HUTECs (A) and primary fibroblasts (B) after stimulation with 1 ng/ml of TGFβ1 for 6 days on a plastic surface; (C) magnification: 400×.

In short, after 6 days of TGFβ1 treatment on collagen, the majority of the fibroblast-like cells were vimentin- and E-cadherin-negative, but still weakly cytokeratin-positive.

In our *in vitro* model, the EMT process driven by TGFβ1 was particularly appreciable at mRNA level after 4 days of treatment.

The close positive correlations observed between TGFβ1 dosage and both cadherin 11 and CTGF expression prompted us to speculate that the other, less closely related dose-dependent events in the EMT process might be secondary events. In particular, as E-cadherin expression was found inversely correlated with cadherin 11, but unrelated to TGFβ1 dosage, we hypothesized that the leading TGFβ1-driven event in the EMT process is cadherin 11 upregulation. Cadherin 11 – the prototype cell–cell adhesion molecule of mesenchymal cells that is strongly expressed in mesenchyme during kidney-branching morphogenesis, or during epithelium-to-mesenchyme induction (Simonneau *et al.* 1995) – was found very recently to mark the molecular phenotype of renal progenitor cells (Challen *et al.* 2004). In the kidney, tenascin also has a crucial role in nephrogenesis, since its expression is restricted to phases of active epithelial growth or movement (Lin *et al.* 1993), particularly expressed in immature nephron structures undergoing mesenchymal-epithelial transdifferentiation (MET). In this context, the TGFβ1-driven upregulation of cadherin 11, MMP-2 and tenascin might be considered as a part of the developmental network's reactivation.

It is also worth dwelling on our finding of a TGFβ1 dose-dependent upregulation of CTGF mRNA, in tubular cells growing on both plastic and collagen. In fibroblasts, proliferation, differentiation into myofibroblasts and increased collagen synthesis are regulated by TGFβ1 via a CTGF-dependent pathway (Grotendorst *et al.* 2004). A recent work by Zhang *et al.* (2004) demonstrated that TGFβ1 drives CTGF upregulation in renal tubular cells too (as we also found), but they also showed that CTGF subsequently upregulated αSMA and fibronectin, thus indicating a crucial role for CTGF in the EMT process leading to myofibroblastic transdifferentiation (TEMT). We found no correlation between CTGF and αSMA or fibronectin expression to suggest a link between CTGF and TEMT, but no myofibroblastic transition was reached in our model. CTGF is also involved in the morphogenic events of kidney development, however, as emerges from the observation that in mouse kidney, CTGF is produced in a specific time- and space-related pattern during embryogenesis, supporting its role in cell differentiation and growth in prenatal life (Surveyor & Brigstock 1999; Stanhope-Baker & Williams 2000). Here again, a reactivation of the developmental network might be suspected in our model of EMT.

As expected, BMP-7 levels were low throughout the EMT process, on both plastic and collagen, thus confirming the endogenous antagonist role of BMP-7 in TGFβ1-induced EMT in the kidney.

Taken together, these data seem to suggest that TGFβ1 makes HUTEC de-differentiate, i.e. it could function as a classic embryonal inducer, initiating a cascade of de-differentiating events that might be further controlled by other factors in the cellular environment.

In our *in vitro* model, TGFβ1 stimulation modulated neither αSMA mRNA nor the αSMA phenotype. Conversely, using quite similar experimental conditions, tubular epithelial–myofibroblast transdifferentiation was induced by treating cells both from a rat kidney tubular cell line (NRK52E) (Fan *et al.* 1999) and from a human proximal tubular cell line (HKC-8) (Yang & Liu 2001).

To gain further insights into how TGFβ1 regulates αSMA in our model, timecourse experiments were performed with 1 ng/ml of TGFβ1 on primary cultures of human fibroblasts and HUTEC, run in parallel under the same culture conditions. One nanogram of TGFβ1 was capable of inducing myofibroblast phenotype in fibroblasts after 6 days of treatment. The same TGFβ1 treatment did not induce the appearance of αSMA microfilaments in HUTEC, although inducing a fibroblast phenotype; indeed, the kinetics of αSMA transcript synthesis were quite different from those of the fibroblasts, in which the treatment caused the αSMA mRNA to double after 24 h, slowly decreasing afterwards. In HUTEC, on the other hand, αSMA mRNA synthesis doubled only after 5 days of continuous exposure. This, however, is not sufficient to trigger myofibroblast transdifferentiation. Even high and unphysiological doses of TGFβ1 induce tubular cells neither to increase their αSMA mRNA content nor to acquire the myofibroblast phenotype. *In vivo*, in experimentally induced kidney obstruction, a robust tubulointerstitial αSMA mRNA induction was obtained only 7 days after surgery (Liu 2004). This may mean that tubular cells are reluctant to undergo myofibroblast transdifferentiation. Indeed, αSMA expression in tubular cells in response to TGFβ1 seems to be very heterogeneous. Even in a homogeneous tubular cell population derived from a single clone, only a small fraction of cultured tubular cells express αSMA protein in response to TGFβ1 stimulation (Iwano *et al.* 2002).

TGFβ signalling pathways downstream from TGFβ receptors are now known in some detail. In this study, we sought to examine the Smad signalling pathway during the EMT process induced by TGFβ1. We found that Smad3 mRNA expression dropped in a dose-dependent manner, while Smad4 mRNA expression was unaffected by long-term TGFβ treatment. Downregulation of Smad3 expression during EMT was

also reported in MDCK cells by Nicolas *et al.* (2003), who suggested that Smad3 plays a crucial part in controlling the cell proliferation triggered by TGFβ1. In particular, the loss of Smad3 function due to a decrease in its expression might be a requirement for epithelial cells to survive in the presence of prolonged TGFβ1 stimulation. In fact, TGFβ1 (the main inducer of EMT) can also promote cell death by apoptosis, so EMT may be the tubular cell's survival mechanism. Cells that escape apoptosis through EMT may potentially serve as a pool of vital cells capable of repopulating the tubular epithelium (regeneration) and/or facilitating repair (myofibroblastic transdifferentiation) (Zeisberg & Kalluri 2004).

Our study results are in line with this hypothesis. In our model, the process triggered by TGFβ1 in HUTEC is a de-differentiation event which might be part of the vital plasticity of renal tubular cells and seems to be similar to that of adult mesenchymal cells, which are long-lived and constantly exposed to the extracellular matrix. The microenvironment provided by the matrix supports both differentiation and the maintenance of a differentiated or undifferentiated state. In other words, this tissue's cell plasticity seems to have the same function as the multipotency of adult stem cells, without needing a real stem cell compartment. It has also been suggested that self-renewal is less crucial for mesenchymal tissue physiology than multipotency and phenotypic flexibility. This implies that commitment and differentiation are reversible in response to environmental cues (Bianchi *et al.* 2001). If this is so, then renal tubular cells – being of mesenchymal origin – might feasibly display, under specific environmental cues, a capacity for interconversion from one cell type to another despite being more mature than adult stem cells. To induce the complete conversion of HUTEC to myofibroblasts, a very complex interaction between ECM components, and growth factors and/or cytokines is most likely necessary.

Acknowledgements

References

Anglani F., Forino M., Del Prete D. *et al.* (1998) Role of epithelial-mesenchymal transformation (EMT) in the acquisition of myofibroblast phenotype during renal fibrogenesis. *JASN* **9**, 512A.

Badid C., Desmouliere A., Babici D. *et al.* (2002) Interstitial expression of alpha-SMA: an early marker of chronic renal allograft dysfunction. *Nephrol. Dial. Transplant.* **17**, 1993–1998.

Badid C., Mounier N., Costa A.M., Desmouliere A. (2000) Role of myofibroblasts during normal tissue repair and excessive scarring: interest of their assessment in nephropathies. *Histol. Histopathol.* **15**, 269–280.

Baer P.C., Tunn U.W., Nunez G., Scherberich J.E., Geiger H. (1999) Transdifferentiation of distal but not proximal tubular epithelial cells from human kidney in culture. *Exp. Nephrol.* **7**, 306–313.

Bianchi G., Muraglia A., Daga A., Corte G., Cancedda R., Quarto R. (2001) Microenvironment and stem properties of bone-marrow derived mesenchymal cells. *Wound Repair Regen.* **9**, 460–466.

Ceol M., Forino M., Gambaro G. *et al.* (2001) Quantitation of TGFβ1 mRNA in porcine mesangial cells by comparative kinetic RT/PCR: comparison with ribonuclease protection assay and in situ hybridization. *J. Clin. Lab. Anal.* **15**, 215–222.

Challen G.A., Martinez G., Davis M.J. *et al.* (2004) Identifying the molecular phenotype of renal progenitor cells. *J. Am. Soc. Nephrol.* **15**, 2344–2357.

Desmouliere A., Geinoz A., Gabbiani F., Gabbiani G. (1993) Transforming growth factor β 1 induces α-smooth muscle actin expression in granulation tissue myofibroblasts and in quiescent and growing cultured fibroblasts. *J. Cell Biol.* **12**, 103–111.

Fan J.M., Ng Y.Y., Hill P.A. *et al.* (1999) Transforming growth factor-β regulates tubular epithelial-myofibroblast transdifferentiation in vitro. *Kidney Int.* **56**, 1455–1467.

Flanders K.C. (2004) Smad3 as a mediator of the fibrotic response. *Int. J. Exp. Pathol.* **85**, 47–64.

Forino M., Murer L., Pagetta E. *et al.* (1997) Alpha smooth muscle actin expression in human renal interstitial cells. *JASN* **8**, 515A.

Friedlander G., Runembert I., Vrtovsnik F., Terzi F. (1999) Renal tubular cells cultured from genetically modified animals. *Exp. Nephrol.* **7**, 407–412.

Grotendorst G.R., Rahmanie H., Duncan M.R. (2004) Combinatorial signaling pathways determine fibroblast proliferation and myofibroblast differentiation. *FASEB J.* **18**, 469–479.

Iwano M., Plieth D., Danoff T.M., Xue C., Okada H., Neilson E.G. (2002) Evidence that fibroblasts derive from epithelium during tissue fibrosis. *J. Clin. Invest.* **110**, 341–350.

Jinde K., Nikolic-Paterson D.J., Huang X.R. *et al.* (2001) Tubular phenotypic change in progressive tubulointerstitial fibrosis in human glomerulonephritis. *Am. J. Kidney Dis.* **38**, 761–769.

Johnson R.J., Floege J., Yoshimura A., Iida H., Couser W.G., Alpers C.E. (1992) The activated mesangial cell: a glomerular 'myofibroblast'? *J. Am. Soc. Nephrol.* **2**, S190–S197.

Lan H.Y. (2003) Tubular epithelial-myofibroblast transdifferentiation mechanisms in proximal tubule cells. *Curr. Opin. Nephrol. Hypertens.* **12**, 25–29.

Lin Y., Kirby J.A., Browell D.A. *et al.* (1993) Renal allograft rejection: expression and function of VCAM-1 on tubular epithelial cells. *Clin. Exp. Immunol.* **92**, 145–151.

Liu Y. (2004) Epithelial to mesenchymal transition in renal fibrogenesis: pathologic significance, molecular mechanism, and therapeutic intervention. *J. Am. Soc. Nephrol.* **15**, 1–12.

Mackensen-Haen S., Bohle A., Christensen J., Wehrmann M., Kendziorra H., Kokot F. (1992) The consequences for renal function of widening of the interstitium and changes in the tubular epithelium of the renal cortex and outer medulla in various renal diseases. *Clin. Nephrol.* **37**, 70–77.

Massagué J. & Wotton D. (2000) Transcriptional control by the TGF-β/Smad signaling system. *EMBO J.* **19**, 1745–1754.

Murer L., Pagetta E., Della Vella M. *et al.* (1998) Expression of intermediate filament in tubular and interstitial cells of obstructed kidneys. *JASN* **9**, 134A.

Ng Y.Y., Huang T.P., Yang W.C. *et al.* (1998) Tubular epithelial-myofibroblast transdifferentiation in progressive tubulointerstitial fibrosis in 5/6 nephrectomized rats. *Kidney Int.* **54**, 864–876.

Nicolas F.J., Lehmann K., Warne P.H., Hill C.S., Downward J. (2003) Epithelial to mesenchymal transition in Madin-Darby canine kidney cells is accompanied by down-regulation of Smad3 expression, leading to resistance to transforming growth factor-beta-induced growth arrest. *J. Biol. Chem.* **278**, 3251–3256.

Oldfield M.D., Bach L.A., Forbes J.M. *et al.* (2001) Advanced glycation end products cause epithelial-myofibroblast transdifferentiation via the receptor for advanced glycation end products (RAGE). *J. Clin. Invest.* **108**, 1853–1863.

Rastaldi M.P., Ferrario F., Giardino L. *et al.* (2002) Epithelial-mesenchymal transition of tubular epithelial cells in human renal biopsies. *Kidney Int.* **62**, 137–146.

Simonneau L., Kitagawa M., Suzuki S., Thiery J.P. (1995) Cadherin 11 expression marks the mesenchymal phenotype: towards new functions for cadherins? *Cell Adhes. Commun.* **3**, 115–130.

Stanhope-Baker P. & Williams R.G. (2000) Identification of connective tissue growth factor as a target of WT1 transcriptional regulation. *J. Biol. Chem.* **49**, 38139–38150.

StrutZ. F., Okada H., Lo C.W. *et al.* (1995) Identification and characterization of a fibroblast marker: FSP1. *J. Cell. Biol.* **130**, 393–405.

Surveyor G.A. & Brigstock D.R. (1999) Immunohistochemical localization of connective tissue growth factor in the mouse embryo between days 7.5 and 14.5 of gestation. *Growth Factors* **17**, 115–124.

Tian Y.C., Fraser D., Attisano L., Phillips A.O. (2003) TGF-beta1-mediated alterations of renal proximal tubular epithelial cell phenotype. *Am. J. Physiol. Renal Physiol.* **285**, F130–F142.

Tosh D. & Slack J.M. (2002) How cells change their phenotype. *Nat. Rev. Mol. Cell Biol.* **3**, 187–194.

Yang J. & Liu Y. (2001) Dissection of key events in tubular epithelial to myofibroblast transition and its implications in renal interstitial fibrosis. *Am. J. Pathol.* **159**, 1465–1475.

Zavadil J., Cermak L., Soto-Nieves N., Bottinger E.P. (2004) Integration of TGF-beta/Smad and Jagged1/Notch signalling in epithelial-to-mesenchymal transition. *EMBO J.* **23**, 1155–1165.

Zeisberg M., Hanai J., Sugimoto H. *et al.* (2003) BMP-7 counteracts TGF-beta1-induced epithelial-to-mesenchymal transition and reverses chronic renal injury. *Nat. Med.* **9**, 964–968.

Zeisberg M. & Kalluri R. (2004) The role of epithelial-to-mesenchymal transition in renal fibrosis. *J. Mol. Med.* **82**, 175–181.

Zhang C., Meng X., Zhu Z., Yang X., Deng A. (2004) Role of connective tissue growth factor in renal tubular epithelial-myofibroblast transdifferentiation and extracellular matrix accumulation in vitro. *Life Sci.* **75**, 367–379.

Zhu M.Q., De Broe M.E., Nouwen E.J. (1996) Vimentin expression and distal tubular damage in the rat kidney. *Exp. Nephrol.* **4**, 172–183.